SEMAIL OPHIOLITE SUPRA-SUBDUCTION ZONE SETTING: EVIDENCE FROM SERPENTINITES AND THEIR CHROMITE AT MUNDASSAH AREA, UAE

El Tokhi, Mohamed
Alaabed, Sulaiman
Amin, Bahaa Eldin
Department of Geology, College of Science,
United Arab Emirates University, Al-Ain, United Arab Emirates

Abstract

Serpentinites as the base of the Semail Ophiolite in the northern United Arab Emirates represent a products of hydration of peridotites as a part of the oceanic lithosphere that was obducted onto the Arabian continental margin during the Late Cretaceous. Three main rock types are recognized in the Mundassah area of eastern UAE: 1-Serpentinized peridotites, 2-Massive serpentinites and 3-Foliated serpentinites. At least three stages of serpentinization are recorded in the Mundassah area. The first stage is characterized by the crystallization of blade-shaped lizardite as pseudomorphic replacement of olivine-orthopyroxene. The second stage is worked by the appearance of fibers and dense fine-grained aggregates of chrysotile and antigorite replacing or cutting the lizardite. The third stage involved crystallization of clinochrysotile and carbonate veinlets.

Analyses of chromite samples from the Mundassah area show that it has relatively high Cr_2O_3 (>53 wt%) and low of Fe_2O_3 (2.9-9.9 wt%) and low TiO_2 (< 0.2 wt%). Mundassah chromites are typical of forearc peridotites and are distinctly different from those of oceanic abyssal peridotites. Most serpentinites have high Cr (>2200 ppm), Ni(>2000 ppm) and MgO (>36 wt%), and low Al_2O_3 (< 2 wt%) and CaO (< 1.5 wt%). Low CaO content may be attributed to the dissolution of clinopyroxene during serpentinization, but very low Al_2O_3 content of together with high Cr suggest that the original rocks were dunite or harzburgite, as this is also suggested by the rock relic texture. For forearc-mantle peridotites, it appears that they were hydrated by the water released from subducted slabs.

Keywords: Semail Ophiolite, Mundassah area, Supra-subduction, Serpentinite and Chromite

Introduction

The United Arab Emirates (UAE) serpentinites are exposed in the anticlinal cores of Jabal Fayah, Jabal Mundassah and Jabal Malaqet. The cores of the Mundassah-Malaqet anticlines are composed of peridotite, serpentinized peridotite and serpentinite that were stacked as thrust sheets before and during folding.

The Jabal Mundassah study area is an appropriate place to study the process of peridotite serpentinization and its relationto the original tectonic setting of the Semail Ophiolite. Some previous workers have described the geological setting, petrology and geochemistry of the peridotites and serpentinites in the Mundassah area (e.g. Osman et al., 2000, 2001). These workers details the PGE contents and chromite chemistry during serpentinization of the ultramafic rocks.

This paper is discussing the tectonic setting of the Semail ophiolite based on evidence from Mundassah serpentinites and it chromite minerals.

2. General Geology

The Semail Ophiolite of Oman and the northern United Arab Emirates is one of the best preserved ophiolites on Earth. It is also one of the largest thrust sheets, with a length of >400 km, a width of 150 km, and an inferred pre-emplacement thickness of 15-20 km (Lippard et. al., 1986). It was emplaced (obducted) onto the Arabian continental margin in the late Cretaceous (98-95 Ma, Albian-Cenomanian) during the closure of the Tethys ocean in the Turonian (~90 Ma) (Lanphere, 1981). The Mundassah area is located SE of AlAin city, in the eastern part of the UAE, and lies at the western margin of the Semail exposures (Fig. 1). The area forms an arcuate belt of post-obduction folds and thrusts, and is represented by a series of regional NNW-SSE trending ridges consisting of a lower ophiolite-mélange assemblage unconformable overlain by Tertiary carbonate sediments.

The Mundassah area is divided into two major units: 1) a lower allochthonous unit including the Hawasina mélange complex, overthrusted by nappes of the Semail Ophiolite (serpentinized peridotite and dunite, and serpentinite); and 2) an upper unit consisting of Cretaceous-Tertiary carbonates, which were deposited after a nappe emplacement. The rock types of Mundassah area consist of: peridotites, serpentinized peridotites and foliated serpentinites, which occur at the core of Malaqet and Mundassah anticlines, and are also found as blocks and pods at Jabal Um Bak and Jabel Al Zarub to the north, but only as a small occurrence of serpentinite along a thrust at its western margin (Fig. 1).

Harzburgite and dunite are predominant rock types of peridotite in the study area. These rocks are massive or foliated and fractured near their contact with the overlying sediments.

The homogeneous and foliated serpentinites are derived from peridotites and contain remnants of this lithology as blocks and lenses. The serpentinized peridotites and serpentinites exhibit horizontal and vertical fractures, mylonitic fabrics and shear foliations. The fractures form a reticulated network of veins filled by iron oxides, green fibrous chrysolite, asbestos, talc and calcite.

The peridotites and overlying carbonates were deformed by NNW-SSE oriented folds and related thrusts. The Malaqet-Mundassah asymmetric anticline is the main structure in the study area. It is cut by two thrust faults - one is parallel to the fold axis and dipping to the east, and the other within the Hawasina mélange complex.

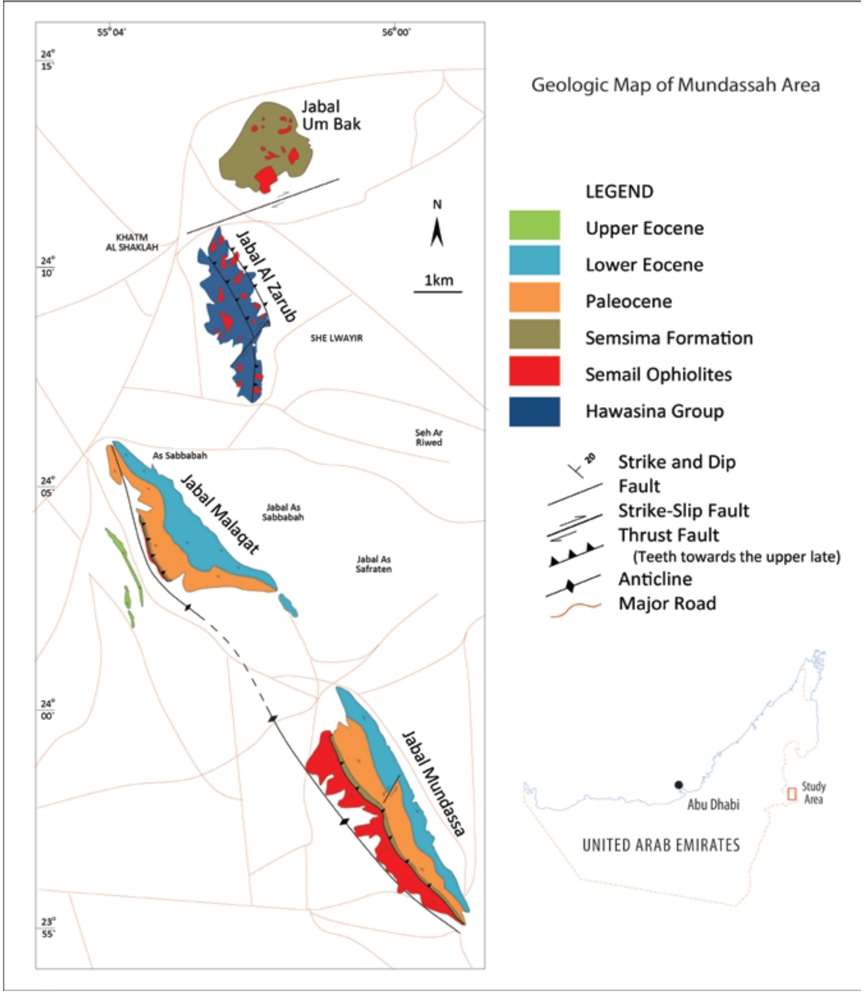

Fig. 1: Geologic map of Jabal Mundassah and Jabal Malaqet

3. Petrography

A detailed petrographic study of the Mundassah meta-ultramafics was carried out by Osman et al. (2001). The following is a brief description of the various serpentinite rocks. The Mundassah serpentinites include massive and sheared varieties. Partly serpentinized peridotite and dunite, chromitite and carbonates occur in subordinate amounts. The massive and foliated serpentinites differ only in fabric. Microscopically, most of the serpentinites consist predominately of lizardite, chrysotile and variable amounts of carbonates, talc, chromite, magnetite, tremolite and chlorite. The Mundassah peridotites rocks can be classified into three types: 1) serpentinized peridotites, 2) massive serpentinites and 3) Foliated serpentinites (Osman et al. 2001).

3.1. Serpentinized peridotites

The serpentinized peridotites are medium- to coarse-grained and show predominantly mosaic texture grading into porphyroclastic textures with large strained orthopyroxene crystals. They consist of olivine crystals up 3 mm in diameter, and variable proportions of orthopyroxene and chromite with subordinate magnetite as well as secondary lizardite, chrysotile, carbonates, talc and tremolite. Chromite forms scattered small subhedral crystals having typically cuspate boundaries. Lizardite has pseudomorphed olivine and orthopyroxene. Chrysotile is commonly present as sets of veins cutting through olivine and pyroxene crystals. Altered pyroxene crystals exist in a serpentinized groundmass forming bastite minerals.

3.2. Massive serpentinites

The massive serpentinites are fine- to medium-grained granoblastic textured rocks composed of lizardite, lesser amounts of chrysotile and antigorite and variable amounts of carbonates, chromite, magnetite, talc and chlorite. Relict olivine and orthopyroxene crystals are present. Olivine is more altered than pyroxene along fractures and grain boundaries. It is converted to mixtures of lizardite and chrysotile forming mesh and hourglass textures..

3.3. Foliated serpentinites

Foliated serpentinites are found adjacent to thrust faults and shear zones in the serpentinized ultramafic rocks as these rocks are high sensitive to alteration (Alaabed, 2011). The intensity of serpentinization and carbonatization increases drastically towards the thrust and shear zones. This alteration is irregular as it is recorded over a distance ranging between a few centimeters to several meters. Foliated and layered serpentinites are composed of lizardite, chrysotile and antigorite together with subordinate carbonates, chlorite and tremolite. Clinochrysotile and carbonate veinlets cut across the lizardite and bastite. Magnetite crystals are scattered throughout the groundmass.

4. Sampling and analytical methods

Eleven rock samples were collected from the study area. Major and minor element concentrations were determined using a Philips PW 2400 X-ray fluorescent spectrometer housed at the Institute of Mineralogy of Karlsruhe University, Germany. Concentrations of the major oxides were obtained on fused lithium-tetraborate discs, while the trace elements were determined on pressed pellets. Loss on ignition (LOI) was determined by heating powdered samples for 50 min at 1000^{o}C. Platinum group elements (PGE) were determined by isotopic dilution technique with a spike of Re and a mixed spike of Pd, Os, Ir and Pt. Rhenium was separated using resin after digestion of samples. PGE pre-concentrated into a Ni bead were dissolved in HNO_3. Mass ratios were determined using a HP4500 inductively coupled plasma mass spectrometer (ICP-MS), at Luleao University, Sweden (the analytical method as described by Ionov et al. 1992). Four concentrates of chromite were analyzed using a Cameca CAMEBX SX 100 microprobe with a counting time of 10s/element, 20 kV accelerating potential, and 20 nA sample current, at Luleao University, Sweden.

5. Geochemistry

5.1. Chromite chemistry

In most of studied samples chromite grains (90-160 µm in diameter) are found to be oxidized to ferrichromite and magnetite, however the cores of a few chromite grains in the Mundassah samples preserve their primary compositions, judging from their low Fe^{3+} (Fe^{3+}/[Fe^{3+} + Al + $Cr^{3+]}$ < 0.12), and TiO_2 (<0.22 wt%; Table 1). The Cr # of chromite is a good indicator of the degree of partial melting for mantle derived peridotites (Dick and Bullen, 1984). Chromite samples of the studied rocks have relatively high Cr_2O_3 (>53 wt %) with variable Cr# (atomic ratio Cr/[Cr + Al]) ranging from 0.79 to 0.84 (Table 1) and low of Fe_2O_3 (2.9-9.9 wt%) and low TiO2 (< 0.2 wt%). Ahmed and Arai (2002) demonstrated the compositional difference between chromites from an early concordant chromitite layer (Cr# = 0.62 and PGE-poor) and chromites from a later, discordant dyke (Cr# = 0.71, PGE-rich) in Wadi Hilti, northern Oman Ophiolite. The chromites of this study have high Cr# (~0.8) due to lower Al_2O_3 (< 9.82 wt %). The Mg# values (atomic ratios of Mg/ (Mg+Fe2+) are similar (0.33-0.39) in all samples. The Cr # of chromite is higher in peridotite restite with a higher degree of partial melt extraction, e.g. in more depleted peridotites. The Cr # value is also useful in discriminating the tectonic setting of peridotites. It has distinguished between chromites derived from abyssal peridotites of mid-ocean ridge setting (Cr # < 0.6) and those from highly depleted harzburgite (Cr # > 0.6) in several parts of the Oman ophiolite (Kanke Takazawa 2005). Figure 2 shows a ternary trivalent cation plot for chromite grains in the serpentinites of the Mundassah study area. All of the samples plotted in the field of forearc peridotites. A plot of Cr# vs. Mg# shows that the samples are similar to those of arc setting (Fig. 3) suggesting a depleted mantle source. Mundassah spinel chromites are distinctly different to those from oceanic abyssal peridotites.

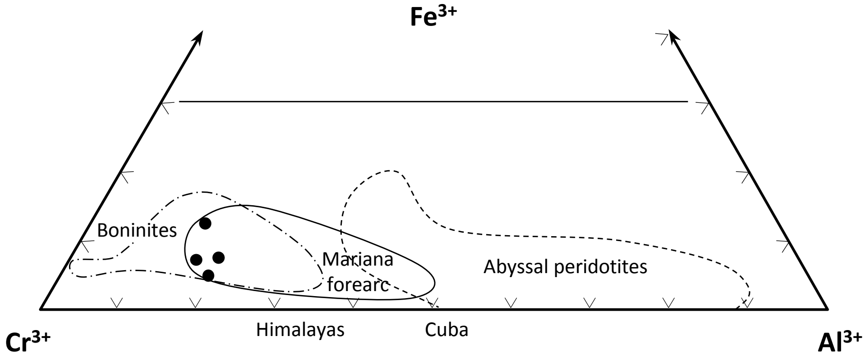

Fig. 2: Ternary trivalent cation plot composition of the cores of chromite grains in serpentinites.

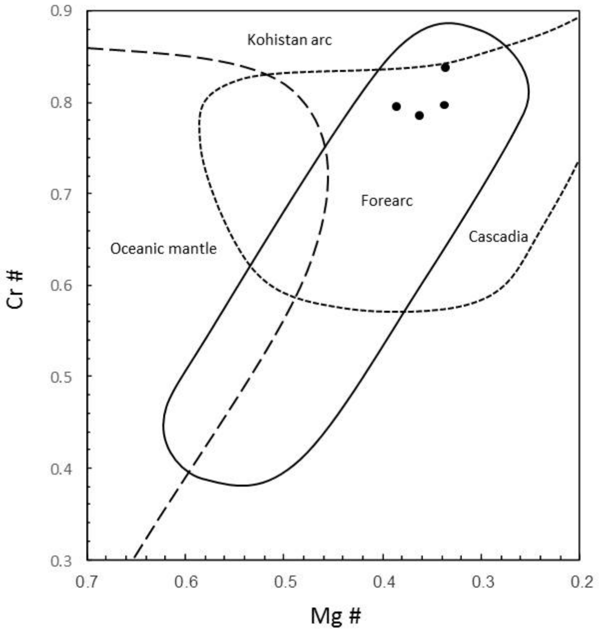

Fig. 3: Composition of chromian Cr # = atomic ratios of Cr/ (Cr+Al), Mg # = atomic ratios of Mg/(Mg+Fe^{+2})

5.2. Whole rock geochemistry

The chemical analyses of Mundassah serpentinites are given in (Table 2). All of the analyzed samples have higher LOI values (10, 15, 17, 45 wt. %) consistent with the hydrous nature of these rocks.. They contain 35 – 40.05 wt. % SiO2, 35.86 – 41.62 wt. % MgO, 0.37 – 1.10 wt. % Al_2O_3 and 6.21 – 8.90 wt. % total iron as Fe_2O_3. Cr and Ni contents are high (2100 - 2770 ppm and 1987 – 2820 ppm, respectively), whereas Co ranges from 95 - 114 ppm. Most of the serpentinites in the study area are characterized by low concentrations of incompatible elements, which are useful in evaluating the origin of igneous rocks. In addition, they contain high concentrations of PGE which may be used to discriminate the origins of serpentinites. Most samples in the Mundassah area contain high Cr (>2200 ppm), Ni(>2000 ppm), and MgO (>36 wt%). Alabeed (2000) found that MgO in the UAE peridotites is higher than the average mantle peridotites value (35 wt% by Taylor & McClennan, 1995) and low Al_2O_3 (< 2 wt%) and CaO (< 1.5 wt%) (Table 2). Low contents of CaO may be attributed to the dissolution of clinopyroxene during serpentinization, but very low contents of Al_2O_3 together with high Cr suggest that the original rocks were dunite or harzburgite (Guillot el al., 2001). On the Al_2O_3 versus CaO diagram (Fig. 4) serpentinites from Mundassah are depleted in Al_2O_3 and CaO and resemble forearc peridotites. The higher Mg # is accompanied by high contents of Ni, Cr and Co and depletion in the incompatible elements reflecting the depleted and high refractory nature of the parent rocks (Roberts, 1992). Moreover, the high Cr # of the chrome chromites combined with the high contents of Ni, Cr and Co in the bulk serpentinites suggest high degrees of partial melting (Ishiwatari et al., 2003). These rocks also contain low concentrations of mildly incompatible elements, such as Ti and V, consistent with their derivation from mantle residues. The Mg# values (atomic ratios of Mg/[Mg + Fe] in bulk rocks) are commonly used to show the degree of depletion after partial melting. Mg# values in upper mantle peridotites in the northern Semail Ophiolite (UAE) range between 0.9 and 0.93 (Alaabed, 2000) and this indicates that the dunites, like harzburgites, are residues of partial melting. The residual mantle origin of the Mundassah serpentinites is confirmed by the plots of Ti/Cr vs. V/Cr and Ti/Cr vs. Al/Cr (Fig. 5).

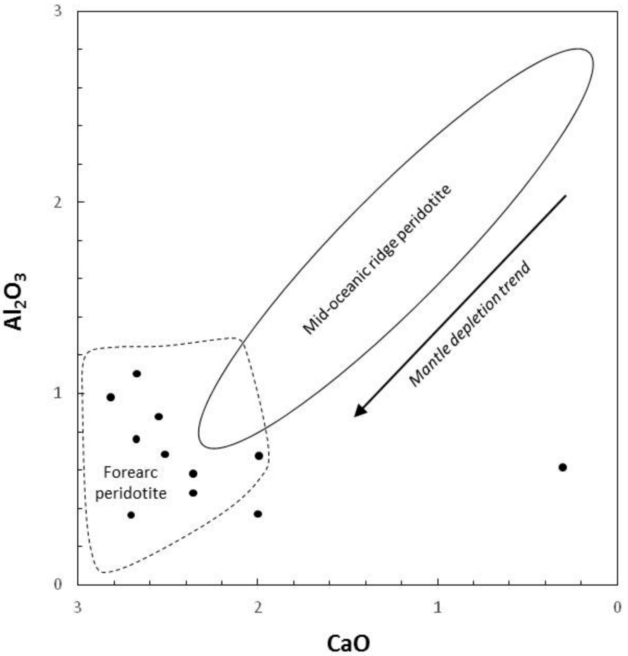

Fig. 4: Al_2O_3 WT % versus CaO WT % diagram for the study serpentinites samples (after Ishii et al 1992).

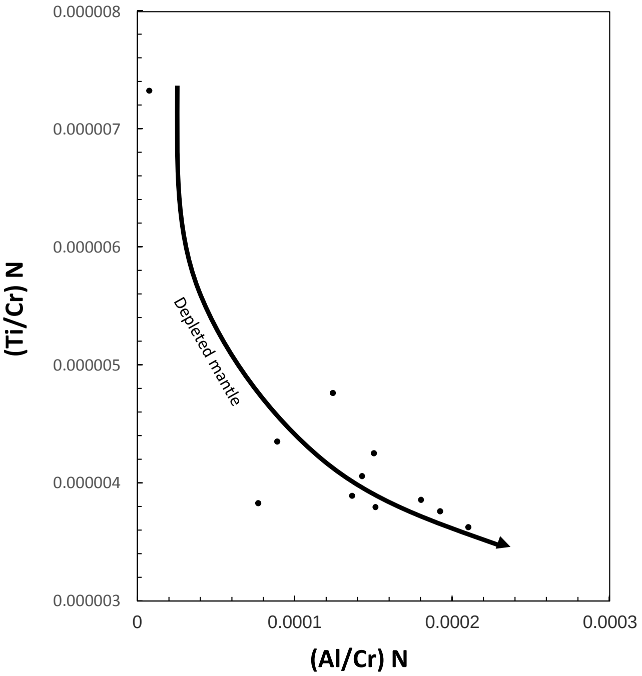

Fig. 5: Primitive mantle-normalized elemental ratio: (Al/Cr) N versus (Ti/Cr) N diagram.

The foliated serpentinites contain a relativity high content of CaO 2.76 wt%, sample 11) and low content of Ni and MgO, consistent with the occurrence of chlorite, carbonate and relict plagioclase. The compositions suggest that they were once solidified melt in the upper most mantle or lower crust. This is further supported by high concentrations of moderately incompatible Ti and V relative to primitive mantle values.

The ratios of Mg/Si and Al/Si appear to provide definitive parameters indicating a primary nature of the protoliths of the peridotites. However, not all major elements are immobile. The CaO is highly mobile, and its depletion is noted in all samples from the Mundassah area. The data suggest that alteration of clinopyroxene is accompanied by dissolution of Ca (Fig. 6).

Table 1: Chromite compositions of the studied serpentinites

Oxides	1	2	3	4	A. Dunite	A. Harzburgite
SiO_2	0.02	0	0	0.03	0	0
TiO_2	0.04	0.04	0.18	0.06	0.13-0.27	0.0-0.11
Al_2O_3	8.8	9.2	6.6	9.8	8.5-20	11.4-28.3
Fe_2O_3	3.79	2.9	9.92	4.4	0.0-6.2	0.0-6.2
FeO	22.93	21.85	23.18	22.16	13.2-19.3	13.5-21.5
MgO	6.71	7.7	6.28	7.39	9.3-13.4	7.8-14
MnO	0.01	0.01	0.01	0.01	0.23-0.97	0.43-1.06
NiO	0.04	0.06	0.06	0.01	0.0-0.19	0.0-0.17
ZnO	0.01	0.17	0.29	0.22	n.d	n.d
Cr_2O_3	57.09	58.7	53.4	55.8	47.5-61.5	42.2-57.2
Total	99.64	100.84	100.13	100.4		
Calc. based on 32 O						
Si	0	0	0	0		
Ti	0.01	0.01	0.04	0.01		
Al	2.85	2.93	2.16	3.12		
Cr	12.36	12.44	11.7	11.94		
Fe^{+3}	0.78	0.58	2.06	0.9		
Fe^{+2}	5.24	4.88	5.31	4.95		
Mg^{+2}	2.75	3.09	2.58	2.96		
Mn^{+2}	0	0	0	0		
Ni^{+2}	0.01	0.01	0.01	0		
Zn^{+2}	0	0.03	0.06	0.4		
Cr#	81	0.81	0.84	0.79	0.62-0.82	0.50-0.77
Mg#	0.34	0.39	0.33	0.38	0.4-0.6	0.38-0.62
X_{Cr}	0.81	0.81	0.84	0.79		
X_{Mg}	0.34	0.39	0.33	0.37		

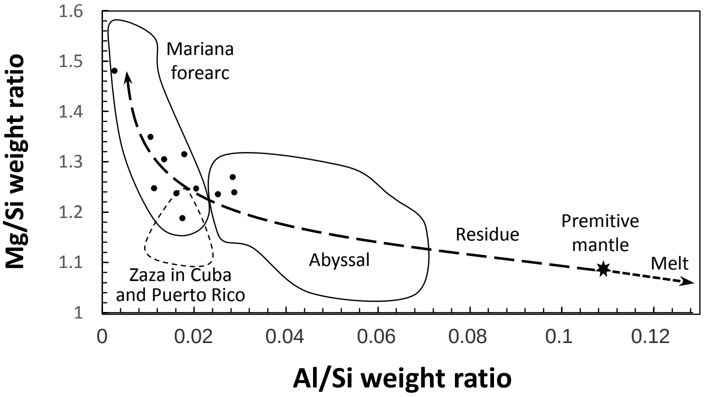

Fig.6: Al/Si weight ratio versus Mg/Si weight ratio diagram for the study serpentinites samples (after Hattori and Guillot, 2007).

Table 2: Bulk chemical composition of serpentines samples

Oxide	1	2	3	4	5	6	7	8	9	10	11
SiO_2	38.48	35	40.05	40.49	39.2	38.17	39	38.76	40.12	39.15	36.76
TiO_2	0.02	0.03	0.01	0.02	0.02	0.01	0.01	0.01	0.02	0.01	0.01
Al_2O_3	0.49	0.54	0.37	0.67	1.1	0.75	0.99	0.89	0.37	0.66	0.65
Fe_2O_3	7.68	6.8	7.44	7.49	8.9	7.1	6.69	7.17	7.57	7.38	6.21
MnO	0.1	0.12	0.1	0.09	0.1	0.11	0.1	0.1	0.09	0.01	0.11
MgO	38.66	40	41.62	36.95	38.29	36.8	37.3	36.76	38.65	37.49	35.86
CaO	0.65	0.64	0.3	1.05	0.33	0.33	0.18	0.44	1.05	0.48	2.76
Na_2O	0.005	0.005	0.005	0.005	0.005	0.01	0.01	0.01	0.01	0.01	0.01
K_2O	0.005	0.005	0.005	0.005	0.005	0.04	0.01	0.04	0.01	0.01	0.04
P_2O_5	0.004	0.005	0.006	0.004	0.001	0.01	0.01	0.01	0.01	0.01	0.01
LOI	13.8	17	10.19	13.1	11.8	16.1	15.07	15.11	12.1	14.5	17.45
Cr	2100	2720	2600	2588	2770	2666	2730	2641	2293	2370	2460
V	27	19	18	35	38	30	42	37	29	28	31
Co	105	95	111	95	115	100	99	101	114	97	95
Zn	48	50	55	30	33	30	50	45	34	44	61
Ni	2200	2250	2820	2260	2390	2051	2000	2081	2063	1987	2010
Ga	<10	<10	<10	<10	<10	<10	<10	<10	<10	<10	<10
Zr	<5	<5	<5	<5	<5	<5	<5	<5	<5	<5	<5
Y	<5	<5	<5	<5	<5	<5	<5	<5	<5	<5	<5
Sr	10	23	13	18	15	13	10	22	17	25	45
Pb	139	441	110	115	333	105	117	131	93	134	99
Th	<10	14	10	10	11	<10	<10	<10	<10	<10	<10
U	<10	30	10	10	16	<10	<10	<10	<10	<10	<10
Ce	0.29	0.37	0.41	0.12	0.09	n.d	n.d	n.d	n.d	n.d	n.d
Nd	n.d	0.058	0.076	0.049	0.041	n.d	n.d	n.d	n.d	n.d	n.d
Sm	n.d	0.019	0.021	0.019	0.019	n.d	n.d	n.d	n.d	n.d	n.d
As	56	75	54	16	145	n.d	n.d	n.d	n.d	n.d	n.d
Sb	6.4	10	10	0.69	10.2	n.d	n.d	n.d	n.d	n.d	n.d
Os	*2.2*	*3.71*	*1.5*	*2.91*	*1.6*	*2.1*	2	*2.66*	*3.17*	*3.23*	*0.08*
Ir	2.25	1.5	2.99	1.4	2.8	2.2	1.94	1.53	2.41	4.23	0.41
Pt	2.1	1.46	6.8	5	5.44	2.1	3.11	1.47	10.51	2.63	1.2
Pd	8.36	2.22	4.59	2.85	10.1	8.35	4.66	2.32	4.47	3.9	10.8
Re	0.013	0.012	0.02	0.027	0.2	0.012	0.017	0.013	0.03	0.028	0.013

5.4. Platinum Group Elements

Platinum group elements (PGE) are divided into two subgroups: Pt-group (Pt, Pd and Rh) and Ir-group (Ir, Os, Ru). The former group of elements may be enriched in melts whereas the later elements are compatible during partial melting and are retained in the mantle. The contents of PGE in the studied area show high concentrations of Os and Ir and low ratios of Pt-group /Ir- group, displaying a flat, primitive mantle-normalized pattern with a depletion of Re and enrichment of Pd (Fig. 7). Several samples show a moderate enrichment of Pd, which may be attributed to serpentinization because Pd is relatively mobile in saline fluids (Boudreau et al., 1986). The concentrations of PGE and ratios of Pd/Ir and Pt/Ir for most of the samples are similar to ultramafic massifs (Gueddari et al., 1996).

The PGE data suggest a mantle origin for the serpentinite samples (Fig.8). As a rule, rhenium is incompatible during partial melting and the concentration of Re in melts is high, even for those derived from a depleted mantle (Roy-Barman and Allegre, 1994). Thus the low Re values suggest that the Mundassah samples represent mantle residues. The samples contain high Os and Ir and low Al, and plot in the field of mantle residue (Fig. 9). In contrast, the highly sheared samples contain low Os and Ir and high Pd and Pt (Table 2). Incompatible Re, Pt and Pd may be enriched in magmas, whereas compatible Os and Ir remain in the mantle. Therefore, crustal rocks are generally low in Os and Ir (Peck et al., 1992).

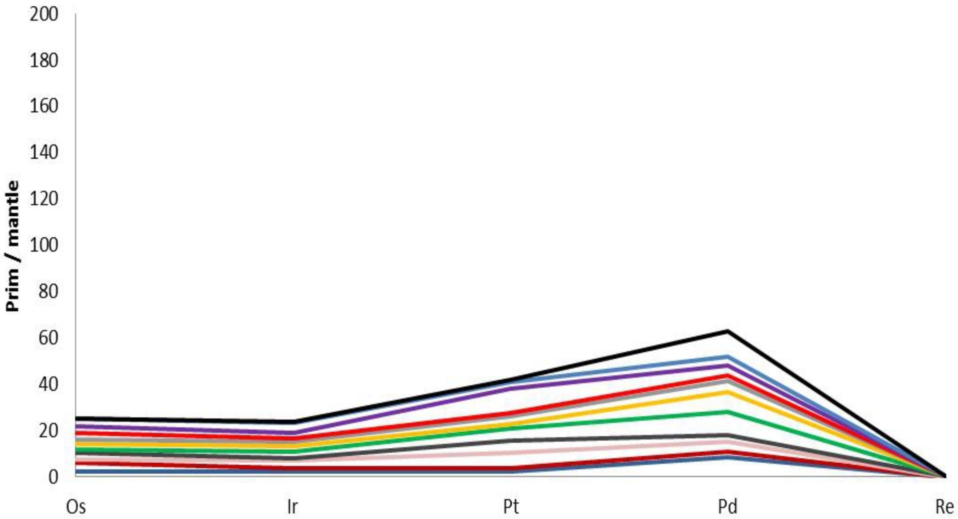

Fig. 7: Primitive mantle-normalized plot of Os, Ir, Pt, Pd & Re contents in the studied serpentinites.

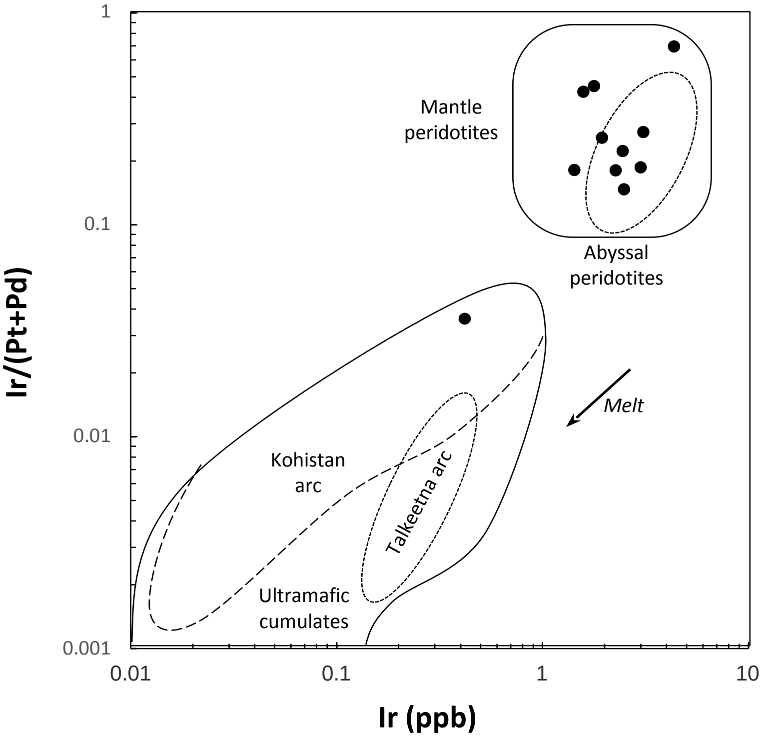

Fig. 8: Ir (ppb) versus Ir/ (Pt+Pd) diagram

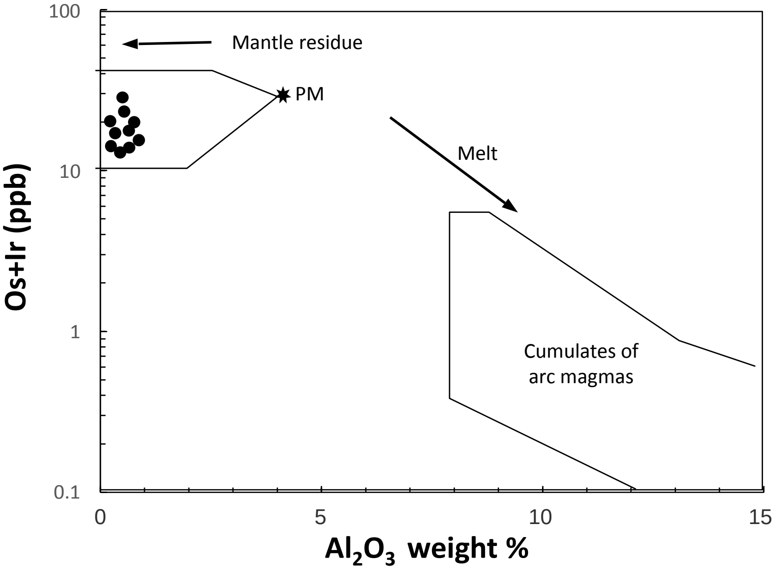

Fig. 9: (Os+Ir (ppb) versus Al_2O_3 of serpentinites samples in the study area (after Hattori and Hart, 1997).

6. Discussion

6.1. Processes and stages of serpentinization

Identifying the parent igneous rocks of serpentinites may be very difficult due to mobilization of many incompatible elements during alteration and metamorphism (Dungan, 1979). However, Boudreau et al. (1986) recognized that serpentinites contain significant amounts of transition elements, which are generally immobile during metasomatism and metamorphism.

Serpentinization can result from more than one process: a) infiltration of seawater into oceanic lithosphere at MOR's via oceanic fractures; b) marine (or sub-aerial) weathering of peridotite that has been exhumed to the surface at fracture zones or low-angle detachment faults; c) infiltration of seawater into extensional faults formed in the zone of bending of a subducting slab; and d) dehydration of subducted or underthrusted oceanic crust followed by fluid fluxing of overlying mantle wedge material.

We refer to serpentinization in scenario b) as an ex situ process, whereas all the other processes are in situ processes, i.e. serpentinization occurring largely in place within the oceanic lithospheric mantle or mantle wedge. A fundamental feature of marine weathered serpentiniztes is their significant depletion in Mg due to dispersion of Mg into the Mg undersaturated seawater (Snow and Dick, 1995). In contrast, the water–rock ratio in the three other scenarios (a, c and d) is likely to be much lower, hence Mg saturation in hydrothermal waters will be reached fairly quickly in a semi-closed system, resulting no significant Mg loss from peridotites. Indeed, the serpentinization process in many ophiolite sections has been shown to be largely isochemical, at least in terms of the major elements (Komor et al., 1985).

Major-element concentrations in the serpentinites of the study area indicate that the Mundassah samples originated from highly refractory peridotites. It is not possible for ex situ serpentinization (scenario b) to have occurred in this case. Serpentinization via b) probably occurs when the exposure time of peridotites on the seafloor is relatively short. We therefore expect that the serpentinization of the Mundassah peridotites was an in situ process.

Lizardite forms the main serpentine mineral in the massive and foliated serpentinites of the Mundassah area. It occurs as large plates bounded by fibrous chrysotile. Lizardite-bastite exists as large grains apparently pseudomorphous after olivine and orthopyroxene, or as mesh-like aggregates indicative of derivation from olivine. Lizardite is a low-temperature phase of the serpentine minerals (Evans, 1977) and is veined or replaced by antigorite and chrysotile in most of the samples. Chrysotile occurs as irregular fibers of variable width, and also replaces the lizardite or bastite of the mesh rims. Antigorite occurs as dense fine-grained aggregates, which were formed by replacement of lizardite and bastite. The textural evidence indicates that the peridotites in the Mundassah area underwent early hydration to form lizardite at low temperatures, followed by a later heating event that formed the antigorite and chrysotile. A final serpentinization stage produced clinochrysotile and carbonate millimeter-wide veinlets that cut through the lizardite-chrysotile-antigorite foliations and crystallized magnesite, talc and magnetite in the shear zones. Neal and Stanger (1984) and Stanger (1986) suggest two types of serpentinization in the Semail ultramafic rocks. The first one " higher temperature alteration serpentinization" is relatively uniform in its effects and unrelated in any way with water tables. It is possible took place either whilst the ophiolite was in situ part of the oceanic lithosphere or during its detachment. . The second type is "low temperature precipitation serpentinization" which related to the movement of present day meteoric waters through the rocks.

The above discussion of textures and serpentine phases points to three stages in serpentinization of the peridotites in the Mundassah area. The first stage is characterized by the crystallization of blade-shaped lizardite as pseudomorphic replacement of olivine-orthopyroxene. The second stage is worked by the appearance of fibers and dense fine-grained aggregates of chrysotile and antigorite replacing or cutting the lizardite. The third stage involved crystallization of clinochrysotile and carbonate veinlets.

6.2. Geochemistry and tectonic setting

The Mundassah peridotites are characterized by enrichments in fluid-mobile elements (LILE's) Cs, Rb, Ba, U, Sr and Li. Both seawater and fluids released during dehydration of a subducting slab are enriched in these elements (Saunders et al., 1980; Gill, 1981; Pearce, 1983), and so the enrichment patterns of normal Mundassah peridotites may be explained either by i) seawater-derived hydrothermal fluid infiltration or ii) slab dehydration related fluid fluxing. It may be possible to distinguish between scenarios i) and ii) on the basis of differents temperatures for the fluids involved in these two cases. In the most likely case that fluids released into the mantle wedge by subducting slabs (case ii) are somewhat hotter than those related to seawater infiltration into lithosphere (case i), a slight enrichment in LREEs (e.g., La, Ce, Pr) relative to HFSEs (e.g., Ti, Nb, Zr and Hf) may be expected in the resulting serpentinites. This is because at temperatures higher than 300°C, small amounts of LREE's may become mobile (Gammons et al., 1996), in contrast to HFSE's, which remain comparatively insoluble in hydrous melts (Saunders et al., 1980; Gill, 1981; Pearce, 1983; Keppler, 1996). As a result, the hotter fluids derived by slab dehydration will generate both LILE and LREE enrichments, as well as apparent depletions in HFSE’s. The overall LREE depleted signatures (compared to HFSE’s) of the average Mundassah serepentinized peridotites indicate that subduction-related fluids were probably not responsible for most of the serpentinization. Thus, based on the seawater signature, conservation of major element compositions (Fig. 2) and low metamorphic temperatures, our preferred interpretation is that the majority of the Mundassah peridotites were serpentinized by seawater while they were structurally in place within the oceanic lithosphere, and not during or after tectonic obduction. We speculate that the Mundassah peridotites were probably serpentinized via fractures or faults in the lithosphere, i.e. serpentinization processes a) and c).

The collective data from the Mundassah serpentinite bulk composition and mineral analysis of chromite grains disseminated within the serpentinites are consistent with modern forearc tectonic settings. Putting this in the regional tectonic framework of the Arabian plate suggests formation of Mundassah serpentinites at the base of a forearc-mantle wedge above descending Neotethys oceanic crust in a supra-subduction zone setting.

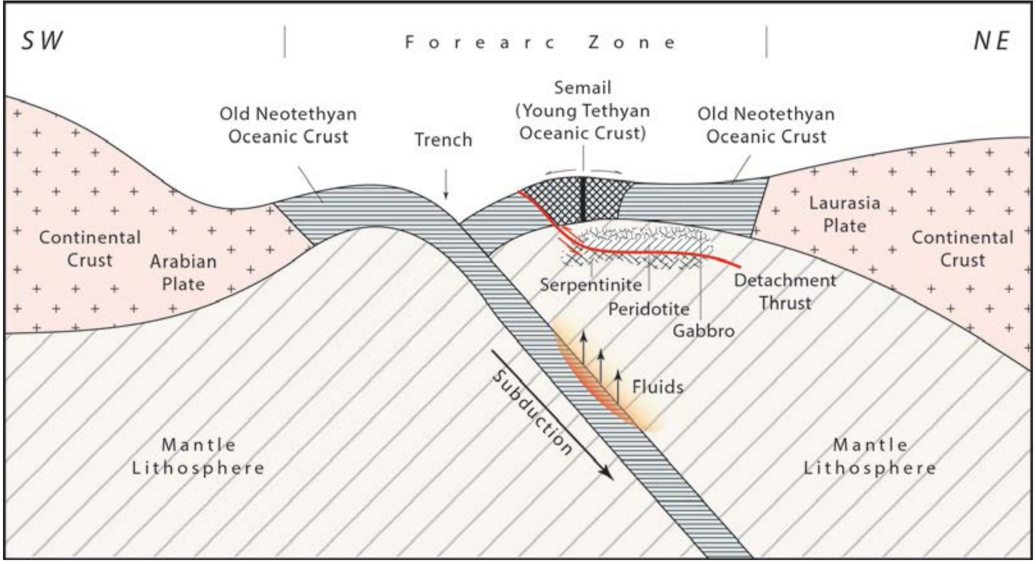

Fig. 10: Mundassah continental margin.

6.3. Source of Water for the Hydration of Peridotites

Serpentinization of oceanic lithosphere is of interest to geoscientists as it forms an essential part of a cycle connecting surface waters with vapours in the upper mantle. This recycling of water has a effect on the dispersion of certain fluid-mobile elements (such as F, Cl and B) during subduction (Leeman, 1996; Straub and Layne, 2003; Rüpke et al., 2004; Sharp and Barnes, 2004)

Serpentinite can be a major component of the upper part of the oceanic lithosphere and is a significant H_2O contributor to subduction zones (Scambelluri et al., 2004). Serpentinite dehydration releases large amounts of water through a very limited number of discontinuous reactions and therefore has the potential to leave distinctive trace element chemical fingerprints in overlying rocks (Ulmer and Trommsdorff, 1995; Scambelluri et al., 2004; see also Pettke et al., 2009).

The sources of water for hydration depend on the tectonic setting of the protoliths of the serpentinites. For forearc-mantle peridotites, it appears that they were hydrated by the water released from subducted slabs. Stanger, 1986 suggest that the all-pervasive serpentinization was produced partly by the passage of sea water. In contrast, the oxygen isotope studies on the Semail mantle sequence (Dunlop and Fouillac, 1984) indicate that the serpentinization was mainly produced by meteoric water at low temperatures (50^{o}C). The fluids originated as meteoric waters and the serpentinization must be related to the post-obduction part of the ophiolite history producing late stage, cross-cutting veins. For abyssal peridotites, the hydration is likely due to seawater, on the evidence that their bulk-rock compositions are typically similar to those of abyssal peridotites, and their associated omphacitic eclogites have the chemistry of oceanic basalts and gabbros. The present study area is characterized by the absence of both oceanic basalt and eclogite.

Abyssal peridotites and oceanic basalts are known to acquire Sr in solution during alteration by seawater, as evidenced by the low contents of Sr in anhydrous peridotites (Kimball and Gerlach, 1986). Other supporting evidence is provided by high 87Sr/86Sr values for serpentinites compared to the upper mantle value (Fig. 9). Most values are similar to the present-day marine Sr value. Considering that there was a lower 87Sr/86Sr ratio in the Paleocene-Eocene sea water than at present (McArthur et al., 2001), a high 87Sr/86Sr ratio suggests a contribution of Sr from abundant sediments, which likely accumulated on a slow-spreading oceanic plate.

7. Conclusion:

Mundassah serpentinites at the eastern border of the UAE form part of the mantle ultramafics of the Semail ophiolite that extends along the northeastern margin of the Arabian plate. The rocks are represented by partially serpentinized and massive serpentinites. Some are strongly foliated by intense deformation. Three stages of serpentinization can be recognized at Mundassah area. The earliest stage resulted in crystallization of bladed lizardite as pseudomorphous grains after olivine and orthopyroxene. The second stage produced fibers and fine dense aggregates of chrysotile and antigorite replacing or veining the lizardite. The third serpentinization stage produce millimeter-wide clinochrysotile and carbonate veinlets cutting through the foliated lizardite-chrysotile-antigorite and magnesite + talc + magnetite replecements in some shear zones.

The geochemical signatures of Mundassah serpentinite (high Cr, Ni, and MgO, and low Al_2O_3 and CaO) and mineral chemistry of their chromites (high Cr_2O_3, and low Fe_2O_3 and TiO_2) are characteristic of forearc mantle peridotites and distinct from oceanic abyssal peridotites. Low contents of CaO may be attributed to the dissolution of clinopyroxene during serpentinization, but very low contents of Al_2O_3 together with high Cr suggest that the original rocks were dunite or harzburgite. Based on the seawater signature, conservation of major element compositions and low metamorphic temperatures, our preferred interpretation is that the majority of the Mundassah peridotites were serpentinized by seawater while they were structurally in place within the oceanic lithosphere, and not during or after tectonic obduction. For forearc-mantle peridotites, it appears that they were hydrated by the water released from subducted slabs. This indicate that the rocks were serpentinized by subduction related fluids in a supra-subduction zone setting.

References:

Agard P, Jolivet L, Goffé B (2001) Tectonometamorphic evolution of the Schistes Lustrés complex: implications for the exhumation of HP and UHP rocks in the Western Alps. Bull. Soc. Geol. Fr. 172 (5), 617–636.,

Ahmed AH, Arai S (2002) Unexpected high-PGE chromitite from the deeper mantle section of the northern Oman ophiolite and its tectonic implications. Contributions to Mineralogy and Petrology 143, 263–78.

Alaabed S (2000) Petrogenesis of chromite and associated minerals in the upper mantle peridotite of the Northern Semail ophiolite (UAE). Ph.D. Thesis. Ohio State University, Columbus, OH USA.

Alaabed S (2011) Rocks Mineralogy Controls the Metasomatic activities: an Indication from Water/Rock Ratio Modeling. *Arab. J. of Geosci.*, Vol.4, No. 1-2, p283-289.

Boudreau AE, Mathez EA, McCallum, IS (1986) Halogen geochemistry of the Stillwater and Bushveld Complexes: Evidence for transport of the platinum group elements by Cl-rich fluids, J. Pet., v. 27, p. 967-986, .

Dick HJB, Bullen T (1984) Chromian spinel as a petrogenetic indicator in abyssal and alpine-type peridotites and spatially associated lavas. Contrib. Mineral. Petrol., 86: 54-76.

Dungan M (1979) A microprobe study of antigorite and some serpentinite psseudomorphs, Can. Mineral. 17 (1979) 771-784, .

Dunlop, H. M. and Fouilac, C. (1984) O, H, Sr, Nd isotope systematics of the Oman Ophiolites. “Through Time”. Conf. Nantes abst. P. 25.

Evans BW (1977) Metamorphism of alpine peridotite and serpentinite.

Annu. Rev. Earth Planet Sci. 5,397-447.

Gammons CH, Wood SA and Williams AE (1996) The aqueous geochemistry of rare earth elements and yttrium: VI. Stability of neodymium chlorite complexes from 25 to 300 degrees C. Geochemica et Cosmochemica Acta, v. 60, p. 4615-4630.

Gill JB (1981) Orogenic Andesites and plate tectonics. Springer-Verlag, New York.

Gueddari K, Piboule M and Amosse J (1996) Differentiation of platinum-group elements (PGEs) and gold during partial melting of peridotites in lherzolitic massif of the Betico-Rifean range (Ronda and Beni Bousera): Chemical geology, v. 134, p.181-197.

Guillot S, Hattori K, De Sigoyer J, Nagler T and Auzende A L (2001) Events of hydration of the mantle wedge and its role in the exhumation of eclogites. Eath Planet. Sci. Lett.193, 115-127.

Hattori KH, Guillot S (2007) Geochemical character of serpentinites associated with high to ultrahigh pressure metamorphic rocks in the Alps. Cuba, and the Himalayas recycling of elements in subduction zones. Geochem. Geophys. Geosyst., 8, Q09010,27 pp.,doi: 10. 1029/2007GC001594,.

Hattori KH, Hart S R (1997) PGE and Os isotopic signatures for ultramafic rocks from the base of the Talkeetna island arc, Alaska: Eos (transaction, American Geophysical Union), v. 78 p.339.

Hofmann AW, Jchum KP, Seufert M, White WM (1986) Nb and Pb in oceanic basalts: New constraints on mantle evolution. Earth Planet. Sci. Lett. 79, 33-45.

Ionov DA, Savoyant L, Dupuy C (1992) Application of the ICP-MS technique to trace element analysis of peridotites and their minerals. Geostandards Newsletters 16 (2),2 .

Ishii T, Robbiinson pt, Maekawa H, Fiske R. (1992) Petrological studies of peridotites from diapiric serpentinites seamounts in the Izu-Ogasawara-Mariana forearc. Leg 125; scientific results, volume 125 College station, Texas, Ocean Drilling Program, p. 445- 463.

Ishiwatari A, Sokolov SD, Vysotskiy SV (2003) Petrological diversity and origin of ophiolites in Japan and Far East Russia with emphasis on depleted harzburgite. Geol. Soc. London Spec. Publ. v. 218, pp. 597-617, .

Kanke N, Takazawa E (2005) Distribution of ultra-depleted peridotite in the Northern Fizh mantle section from the Oman ophiolite. Abstract for Japan Earth and planetary Science Joint Meeting. pp. 1004-11029, .

Keppler H (1996) Constraints from partitioning experiments on the composition of subduction zone fluids. Nature 380, 237 – 240, .

Kimball KL, Gerlach DC (1986) Sr isotopic constraints on hydrothermal alteration of ultramafic rocks in two oceanic fracture zones from the South

Atlantic Ocean. Earth and Planetary Science Letters 1986; 78:177-188.

Komor SC, Ethon D, Casey JF (1985) Mineralogic variation in the layered ultramafic cumulate sequence at the North Arm Mountain Masif, Bay of Island ophiolite, Newfoundland. Journal of Geophysical Research, 90 (89), 7705 – 7736.

Lanphere MA (1981) K- Ar ages of metamorphic rocks at the base of the Samail ophiolite, Oman. Journal of Geophysical Research 86, 2777---2782.

Leeman WP (1996) Boron and other fluid-mobile elements in volcanic arc lavas: Implications for subduction processes. In: Bebout, G.E., Scholl, D., Kirby, S., and Platt, J.P. (eds.), Subduction Top to Bottom, American Geophysical Union Monograph, 96, 269-276.

Lippard SJ, Shelton AW, Gass IG (1986) The ophiolite of northern Oman. Geological Society London Memoir, 11, 178 p.

McArthur JM, Howarth RJ and Bailey TR (2001) Strontium isotope stratigraphy: LOWESS version 3: best fit to the marine Sr-isotope curve for 0–509 Ma and accompanying look-up table for deriving numerical age. J. Geol., 109:155–170.

Neal, C. and Stanger, G. (1984) Calcium and magnesium hydroxide precipitation from alkaline groundwater in Oman, and their significance to the process of serpentinization. Min. Mag. 48, 237-241.

Noll PD Jr, Newsom HE, Leeman WP, Ryan JG (1996) The role of hydrothermal fluids in the production of subduction zone magmas; Evidence from siderophile and chalcophile trace elements and boron. Geochim. Cosmochim. Acta 60, 587-611.

Osman A.F., Mohamed FH, Amin BM (2001) Progressive serpentinization of some ultramafics in Semail Ophiolite, MundassahMundassah Range, United Arab Emirates. MERC. Ain Shams Univ. Earth sci. Vol. 15.

Osman A.F., Mohamed FH, Amin BM (2000) Petrological and Geochemical Studies on some serpentinites of the Semail Ophiolite, MundassahMundassah Range, United Arab Emirates. 5th Int. conf. on the geology of Arab World, Egypt. 85-86.

Pearce JA (1983) The role of sub-continental lithosphere in magma genesis at destructive plate margins. In: Hawkesworth, C. J., Norry, H. J. (Eds.), Continental Basalts and Mantle Xenoliths. Shiva, Nant-wich, pp. 230-249.

Peck DC, Keays RR, Ford RJ (1992) Direct crystallization of refractory platinum-group elements alloys from boninitic magmas: evidence for western Tasmania: Australian Journal of Earth Sciennces, v. 39,p. 373-387.

Peter Ulmer, Volkmar Trommsdorff (1995) Serpentine Stability to Mantle Depths and Subduction-Related Magmatism, Science Magazine, Vol. 268 no. 5212 pp. 858-861.

Pettk T, Spandler C, Kodolanyi J, Scambelluri M (2009) The chemical signatures of progressive dehydration stage in subduction serpentinites. Vol.

11, EGU2009-9697-1.

Roberts S (1992) Influence of partial melting regime on the formation of ophiolitic chromite. In: Person, L.M., Murton, B.J., Browning, P. (Eds). Ophiolites and their Modern Oceanic Analogues. Geological Society, Special Publication. 6, pp.203-217.

Roy-Barman M, Allegre C J (1994) 187Os/186Os ratio of mid-ocean ridge basalts and abyssal peridotites: Geochemica et Cosmochemica Acta, v. 58, p. 5043-5054.

Rüpke LH, Morgan JP, Hort M and Connolly JAD : Serpentine and the subduction zone water cycle. Earth and Planetary Science Letters, Volume 223, 2004, Pages 17-34, (2004).

Saunders AD, Tarney J, Weaver S D (1980) Transverse geochemical variations across the Antarctic Peninsula: Implications for the genesis of calc-alkaline magmas. Earth and Planetary Science Letters, Volume 46, Issue 3, February 1980, Pages 344-360.

Scambelluri M, Fiebig J, Malaspina N, Müntener O, Pettke T (2004) Serpentinite Subduction: Implications for Fluid Processes and Trace-Element Recycling. Int Geol Rev 46: 595-613.

Sharp ZD, Barnes JD (2004) Water-soluble chlorides in massive seafloor serpentinites: a source of chloride in subduction zones. Earth and Planetary Science Letters, Volume 226, Issues 1-2, 30 September 2004, Pages 243-254.

Snow JE, Dick HJB (1995) Pervasive magnesium loss by marine weathering of peridotite. Geochemica Et Cosmochemica Acta 59 (20),4219-4235.

Stanger, G. (1986) The hydrogeology of Oman Mountains. Unpubl. Ph. D. Thesis, open University, 572 pp.

Straub SM, Layne GD (2003) Decoupling of fluids and fluid-mobile elements as recorded in halogen-rich andesite melt inclusions from the Izu volcanic arc. Geochem Geophys Geosys (Article, Theme: Trench-To-Subarc) 4 (7): 9003, doi:10.1029/2002GC000349, .

Ulmer P, Trommsdorff V (1995) Serpentine stability to mantle depth and subduction related magmatism. Science, 268, 858 – 861.